Chapter 14

Multifunctional Wound-Dressing Composites Consisting of Polyvinyl Alcohol, Aloe Extracts and Quaternary Ammonium Chitosan Salt

Yang Hu, Yongjun Zhu and Xin Zhou

Additional information is available at the end of the chapter

http://dx.doi.org/10.5772/65476

Abstract

Wound dressings are materials generally made of gauze, synthetic, and natural polymers that are able to protect wound from microorganism, absorb exudates, and provide compression to minimize edema as well as a temporary substrate for tissue cells to grow. The multifunction of wound dressing exhibiting antibacterial and anti-inflammatory properties and conducive to skin-tissue regeneration is highly desired. In this study, we developed such a multifunctional wound-dressing composite consisting of polyvinyl alcohol, aloe extracts, and quaternary ammonium chitosan salt (PVA/AE/QCS, PAQ). The mass ratio of PAQ composites was controlled at three different levels of 6:3:1, 7:2:1, and 8:1:1. The as-prepared PAQ composites exhibited a porous profile on both surface and cross-section areas with 3–60-μm pore size and a three-dimensional (3D) porous network inside. Such a porous structure could effectively prevent the invasion of microorganism, as well as readily absorb extrudes from wound. The PAQ composites exhibited a good competency of moisture maintenance, excellent antibacterial characteristics, and a good biocompatibility of fibroblasts, and they would become a competitive multifunctional wound dressing.

Keywords: wound dressing, aloe extracts, chitosan, antibacterial, moisture maintenance

1. Introduction

The occurrence of wound is a cause of break in the skin that generally results from physical, mechanical, and thermal damage, or medical surgery and physiological disorder [1]. It

accompanies cell death, destruction of extracellular connective tissue components, and loss of blood vessel integrity [2]. Wound healing is a dynamic process including inflammatory, proliferative, and remodeling phases. Each phase involves numerous biochemical activities and is overlapped with other phases until the completion of wounded-tissue regeneration [3]. When serious tissue injuries can hardly heal themselves, human interventions are required [4]. The use of wound dressings is such a first step of human interventions to first contribute the hemostasis and prevent wound from deteriorating. Wound dressings are materials generally made of gauze, synthetic, and natural polymers that are able to control moisture content, provide gaseous permeability, protect wound from microorganism, absorb exudates, exhibit low adherence, and provide compression to minimize edema as well as a temporary substrate for tissue cells to grow [1, 5]. Different types of wound need separate wound dressings exhibiting different functions according to various healing objectives. In order to obtain optimal healing result, wound dressings containing integrated functions such as antibacterial and anti-inflammatory properties, and contribution to skin-tissue regeneration are highly desired.

Inorganic materials generally used in wound healing can be selected from a wide range of materials, such as silicone-based bioglasses. Most of them exhibit either high-elastic module satisfying the mechanical requirement of skin tissue or certain biodegradability to release beneficial elements for wound care, such as borate or siloxane bioglasses [6, 7]. Polymeric materials are contributed to most of wound-dressing materials because of their processibility, moldability, low toxicity, biocompatibility, and low cost [8]. Both synthetic and natural polymers can be used to prepare appropriate wound dressings. Some typical synthetic polymers, such as polypropene (PP) and polylactic acid (PLA), although showing excellent molding ability and certain biodegradability, present inadequate biocompatibility and unpleasant side effects [9–13]. Naturally generated polymers are derived from biomacromolecules such as alginate, chitin/chitosan, gelatin, heparin, collagen, chondroitin, fibrin, keratin, silk fibroin, and bacterial cellulose (BC), and most of them show desirable properties of biocompatibility, biodegradability, nontoxicity, fluid exchange, and moldable prototypes during the synthetic process [14–20], although some unavoidable defects, such as high cost, inappropriate mechanical properties, and untunable biodegradability, are still present [14, 21]. Therefore, blending or compositing synthetic polymers with natural polymers using facile but advanced technologies [22] is highly recommended to integrate advantages of both synthetic and natural polymers and minimize their disadvantages for wound care and other medical uses.

Chitosan is the deacetylated derivative of chitin that is a linear polysaccharide composed of β-1,4-D glucosamine and β-1,4-D-N-acetylglucosamine [23]. Due to numerous amino groups, chitosan becomes a significant polysaccharide carrying positive charges. Such a character offers chitosan an impressive antibacterial property because negatively charged cytoplasmic membrane is neutralized by positive charge which leads to the destruction of the function of bacterial cell membrane [24]. Meanwhile, many studies have also demonstrated the effectiveness of chitosan in wound care that specifically exhibits merits in providing the hemostasis, accelerating the fibroblastic synthesis of collagen, and promoting the tissue regeneration [25]. Due to relatively high cost and difficulties in fiber/film forming as compared to the traditional

http://dx.doi.org/10.5772/65476

gauze-type wound dressing, incorporating chitosan as one of active components of wound care into cheap and easily processible material substrates has become an alternative to prepare wound dressing. The typical examples are electrospinning chitosan with polyethylene oxide (PEO) [26], polyvinyl alcohol (PVA) [27], and (PLA) [28], respectively, for antibacterial application and scaffold construction to promote tissue regeneration. Additionally, blending chitosan with other biomacromolecules, such as collagen [29], pullulan [30], and BC [31], can synergetically contribute to the enhancement of biocompatibility and reduce the toxicity of chitosan to normal tissue cells.

Aloe (*Aloe vera*) is a succulent plant and its extracts mainly consisting of carbohydrates and glycoproteins have been found to contribute to the anti-inflammatory and wound-healing activity [32]. The most beneficial effect of Aloe extracts (AEs) is its function in healing burned wound in which the instant reduction of painful feeling may be easily attained [33, 34]. In addition, AE can be added as a bioactive agent to other material substrates and combine other bioactive agents such as curcumin to exert a synergistic function of moisture maintenance, antibacterial, and anti-inflammation, and thereby promote the wound healing [35]. Nowadays, AE has been successfully commercialized and found in many consumer products for either cosmetic or medicinal purposes.

Although the combination of CS and AE has shown the advantage in wound healing, the effectiveness of modified chitosan combining AE as bioactive agents of wound healing incorporated into PVA matrix has not been investigated yet. Therefore, we aimed to develop such a multifunctional wound-dressing composite consisting of PVA, AE, and quaternary ammonium chitosan salt (QCS, 3-chloro-2-hydroxypropyl trimethylammonium chloride-functionalized chitosan) which was expected to exhibit antibacterial property, ability of moisture maintenance, and good biocompatibility for the growth of skin tissue. Three different mass ratios of QCS, AE, and PVA were selected to investigate the effectiveness of wound-dressing composites prepared. Material characterization of as-prepared wound-healing composites was performed to investigate the porous profile, functional groups of materials, thermal stability, and water absorbability. Cell culture study and antibacterial essay were conducted to investigate the antibacterial activity and biocompatibility in an in vitro wound-healing environment.

2. Materials and methods

2.1. Materials

Quaternary ammonium chitosan salt (QCS, 3-chloro-2-hydroxypropyl trimethylammonium chloride-functionalized chitosan, HACC-101) was purchased from Tianhua Bioagents (Dongying, Shangdong, China). Aloe extracts (AE, lyophilized powder, FBE013) were purchased from Five Brothers Bioproducts (Haikou, Hainan, China). Poly(vinyl alcohol) (PVA, 341584 Aldrich) was purchased from Sigma-Aldrich (Saint Louis, MO, USA). All the chemicals were received as it is and used without further purification. L929 mouse fibroblast cells (ATCC CCL-1), human fibroblast cells (HFCs, ATCC CCL110), and *Staphylococcus aureus* (*S. aureus*, ATCC

9213) were purchased from the American-Type Culture Collection (Manassas, VA, USA). *Escherichia coli* (*E. coli*, Trans5α) was purchased from Transgen Biotech (Beijing, China).

2.2. Preparation of QCS/AE/PVA composites

An amount of PVA, AE, and QCS was dissolved in deionized (DI) water with a final concentration of 5% (m:v). The mass ratios of PVA, AE, and QCS in the PVA/AE/QCS (PAQ) mixture were selected at three levels which were 6:3:1 (PAQ1), 7:2:1 (PAQ2), and 8:1:1 (PAQ3). The mixture was poured into a mold with a depth of 0.5 mm and kept at 4°C for 4 h. The cold mixture was then frozen at -20°C for 4 h following a defrozen operation at room temperature for 4 h. This freezing-defreezing operation was repeated three times until a homogeneous gel was achieved. Next, the gel was lyophilized and cut into an identical size for next studies.

2.3. Material characterization by SEM, FTIR, TGA

PAQ composite samples prepared in the last section were coated with gold and then were imaged by the scanning electron microscopy (SEM, FEI Nova NanoSEM450, USA) operating at 5 kV. Both surface and cross section of samples were examined by SEM. Examination of Fourier transform infrared spectroscopy (FTIR, Bruker Vertex 70, USA) spectra for all composite samples was performed under conditions that FTIR data were taken from 500 to 4000 cm^{-1}. OMNIC software (Thermo Electron Corporation) was used to correct and normalize the baseline of FTIR spectra. Thermogravimetric analyses (TGA) of all composite samples were performed by the TGA Q600 (TA Instrument, USA). Thermograms of samples were recorded between 36 and 600°C at a heating rate of 10°C/min and a nitrogen flow of 100 mL/min. TA Universal Analysis 2000 (TA Instrument, USA) was used to calculate the percentage of weight loss, the first derivatives of the thermograms (DTG), and the decomposition temperatures.

2.4. Water absorbability

The lyophilized PAQ composite samples were soaked in phosphate-buffered saline (PBS, pH 7.4) and acetic acid/sodium acetate buffer (HAc-NaAc, pH 5.0). At different assigned times, the sample was taken out and the excessive solution on the surface of the sample was removed by Kimwipes. The water absorbability was the ratio of weight difference of lyophilized sample before and after the soaking versus the weight of lyophilized sample (the amount of adsorbed water vs. dry weight of lyophilized sample).

2.5. Antibacterial assays

E. coli and *S. aureus* were activated and diluted to the desired concentration of 10^8 CFU/mL (CFU is an abbreviation of colony-forming unit). The inoculum of 10 μL *E. coli* and 10 μL *S. aureus* was separately added to the 1-L growth broth consisting of 30-g tryptic soy broth (BD 211825) and 1-L DI water. Two broth media were shaken at 37°C overnight. The bottom-layer media were taken and rinsed by sterile PBS via the centrifugation at 4000 revolutions per minute (rpm) for 3 min, and the rinsing process was repeated three times. The bacterial pellets obtained for two bacteria were re-dispersed, respectively, in the fresh growth broth

http://dx.doi.org/10.5772/65476

and then adjusted to achieve 0.1 of optical density (OD) value for bacterial media (equal to 10^8 CFU/mL). The composite materials prepared were cut into identical round size with a diameter (D) of 10.5 mm. One piece of sample was placed into 12-well culture plate and UV sterilized for 1 h. Each bacterial medium of 16 μL was dripped onto the sample and another piece of sample was immediately covered on the bacterial medium. The culture plate with samples and bacterial media was cultivated at 37°C for 2 h. Next, the samples and the culture plate were rinsed by sterile PBS at least three times. The collected bacterial solution was centrifuged at 4000 rpm for 3 min and the bacterial pellet was re-dispersed in 250-μL fresh broth. The as-prepared bacterial medium of 100 μL was taken and spread out on the agar medium consisting of 40 g of tryptic soy agar (BD 236950) in 1-L DI water. The bacteria with the agar medium were cultivated at 37°C for 15 h. The number of bacteria growing on the agar was counted. The antibacterial ability was calculated according to Eq. (1).

$$\text{antibacterial ability}(\%) = \frac{\text{CFU}_{\text{blank}} - \text{CFU}_{\text{composite}}}{\text{CFU}_{\text{blank}}} \times 100 \quad (1)$$

where $\text{CFU}_{\text{blank}}$ is the number of bacterial colonies growing on the agar medium without the presence of composite samples and $\text{CFU}_{\text{composite}}$ is the number of bacterial colonies growing on the agar medium in the presence of composite samples.

2.6. Biocompatibility

The effect of the composite samples on the proliferation of L929 mouse fibroblast was first examined. The composite samples of 10.5-mm D round size were sterilized under UV light for 1 h and then activated in the α-minimum essential media (α-MEM, ThermoFisher 11095072) at 37°C and 5% CO_2 for 24 h. The activated samples were placed in a 12-well culture plate and 100 μL of activated L929 cells (20,000 cells/mL/well) was then added to the culture plate. The growth media were exchanged to α-MEM plus 10% of fetal bovine serum (FBS, ATCC 30-2021, USA) and added to the culture plate. The cultivation was conducted at 37°C and 5% CO_2 for 5 days. At days 1, 3, and 5, the culture medium in the culture plate was taken out and rinsed by sterile PBS via centrifugation at 120× g relative centrifugal force (RCF), respectively. The collected cell pellet was added to the cell-counting kit-8 (CCK-8, Sigma 96992, USA) consisting of 10% CCK-8 plus 90% α-MEM. The cell mixture was cultivated at 37°C and 5% CO_2 for 2 h and then OD value of cell mixture was examined by ultraviolet-visible (UV-VIS) spectrometry (Shimadzu UV-3600, Japan).

For the cell attachment and morphology of HFCs on the composite samples, HFCs were first activated according to the protocol described in our previous study [18]. The complete growth medium of HFCs was composed by Eagle's minimum essential medium (EMEM) (ATCC 30-2003, USA) plus 10% of FBS. The composite samples were sterilized under UV light for 1 h and then activated by growth medium of HFCs in a 16-well culture plate. Next, the initial cell suspension (2000 cells/mL/well) was added directly onto the samples following the addition of adequate growth medium to each well, and the cultivation was conducted at 37°C and 5%

CO_2. At the assigned day, the culture medium was removed and the attached cells on the samples were rinsed by PBS. The samples were subsequently fixed with 2.5% glutaraldehyde PBS solution at room temperature for 2 h and stained by a small drop of fluorescent isothiocyanate dye (FITC) at 4°C for 1 h. Laser scanning confocal microscope (LSCM, Leica SD AF) with an excitation wavelength of 488 nm was used to examine the cell attachment and morphology.

3. Results and discussion

3.1. Material characterization and water absorbability of wound-dressing composites

SEM images in **Figures 1** and **2** show distinct surface and cross-section morphologies of PAQ composites prepared at different mass ratios of components. Overall, the PAQ composites display a porous morphology and the cross-section images reveal a three-dimensional (3D) porous network inside PAQ composites. It is noticed that the difference lies in the pore size in each composite. Due to the addition of different amounts of AE and QCS, the PVA fibers inside the 3D structural network are covered by AE and QCS. The pore size of 20–30 μm in PAQ2 appears to be more homogeneous on the surface and cross-section areas than PAQ1 and PAQ2. The PAQ1 exhibits smaller pore size of 5–20 μm and the PAQ3 exhibits larger pore size of 20–60 μm. Too smaller pore may inhibit the air exchange and too larger pores may not effectively prevent the adverse microorganism from infection to wound [36]. In order to prepare a satisfactory wound-dressing material, the porous profile of PAQ2 with a mass ratio of PVA:AE:QCS (7:2:1) seems more qualified.

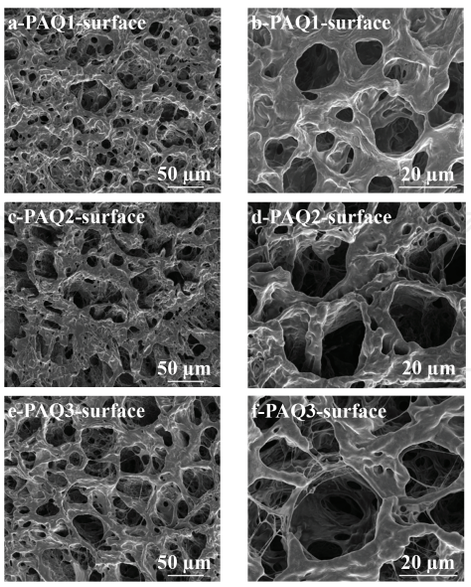

Figure 1. SEM images of surface of PAQ composites with different mass ratios of components: (a, b) PVA:AE:QCS = 6:3:1; (c, d) PVA:AE:QCS = 7:2:1; (e, f) PVA:AE:QCS = 8:1:1. Images b, d, and f indicate higher magnifications of images a, c, and e, respectively.

http://dx.doi.org/10.5772/65476

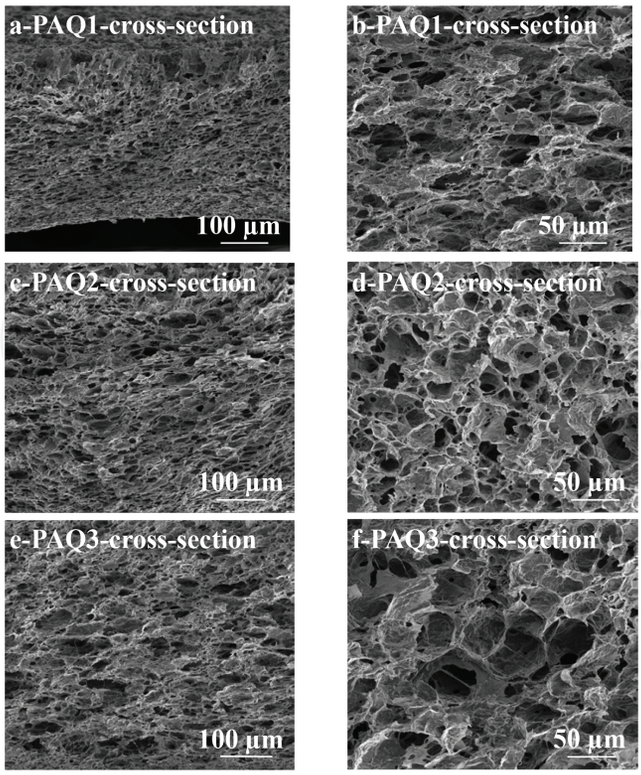

Figure 2. SEM images of cross-section of PAQ composites with different mass ratios of components: (a, b) PVA:AE:QCS = 6:3:1; (c, d) PVA:AE:QCS = 7:2:1; (e, f) PVA:AE:QCS = 8:1:1. Images b, d, and f indicate higher magnifications of images a, c, and e, respectively.

The FTIR spectra of pure PVA, AE, QCS, and PAQ composite samples are illustrated in **Figure 3**. Vertically numerical peaks at 3433 and 2908 cm^{-1} on the pure PVA spectrum may be typical characters of hydroxyl groups and alkyl long chain of PVA, respectively [37]. The strong peak at 3433 cm^{-1} indicates the proof of numerous existing interchain and intrachain hydrogen bonds in the samples of AE and QCS [38]. This peak in three PAQ composite samples shows a limited enhancement as compared to PVA and a remarkable reduction as compared to AE and QCS, suggesting that AE and QCS have been physically bound to PVA and possible hydrogen bonding may have been formed among them. PAQ1 shows a stronger peak at 3433 cm^{-1} than PAQ2 and PAQ3 because of the highest AE component in its composition. The peaks at 1485 and 1230 cm^{-1} are associated with amino groups and they slightly shift to 1400 and 1200 cm^{-1} with the reduction of peak intensity in PAQ composite samples, which is the proof of the presence of QCS in the composites [39, 40]. The strong peaks at 1722 and 1624 cm^{-1} are associated with carbonyl groups existing in AE and they are both present in PAQ composites with the reduction of peak intensity, which is another proof of the incorporation of AE into PVA [40]. The peak at 1120 cm^{-1} is associated with ether groups representing the presence of sugar rings in the PAQ composites, suggesting the successful binding of AE and QCS onto the PVA substrate [40]. The above FTIR analysis chemically demonstrates that AE and QCS have been bound to PVA matrix, although the ratio of AE and QCS in the composites is far below PVA, and as-prepared PAQ composites exhibit all characteristic peaks regarding specific functions that AE and QCS possess.

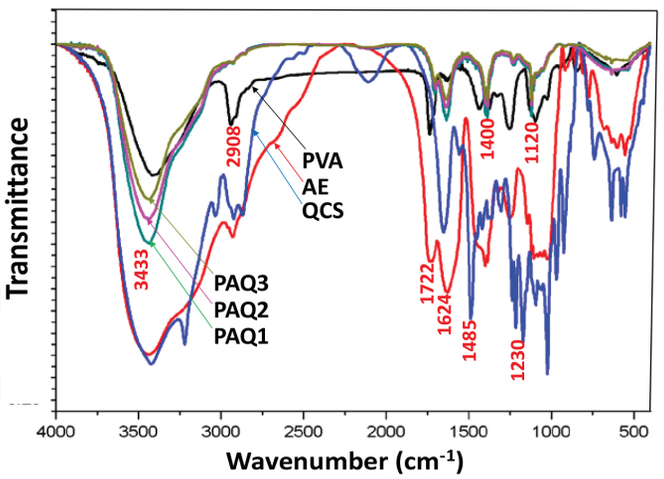

Figure 3. FTIR spectra of pure PVA, pure Aloe, pure QCS, and PAQ composites with different mass ratios of components: PAQ1, PVA:AE:QCS = 6:3:1; PAQ2, PVA:AE:QCS = 7:2:1; PAQ3, PVA:AE:QCS = 8:1:1.

The TGA thermograms of pure PVA and PAQ composites are shown in **Figure 4a** and DTG curves regarding the maximum decomposition temperature and decomposition rate of material components are shown in **Figure 4b**. All the samples show four stages of weight loss in **Figure 4a**. The first stage between 36 and 100°C is associated with the weight loss of absorbed water of samples [19]. Pure PVA exhibits around 8% weight loss in this stage as compared to 9.82% for PAQ3, 15.42% for PAQ2, and 18.51% for PAQ1, suggesting that the competency of moisture maintenance of PAQ composites increases according to the increasing content of AE and QCS in the composition. The second stage between 150 and 300°C is associated with the disintegration of intermolecular breaking of molecular structure which is believed to be the disassociation of physical binding among material components [41]. In this stage, the weight losses of composites are around 25% for pure PVA, 27.25% for PAQ3, 30.36% for PAQ2, and 29.91% for PAQ1, which suggests that AE and QCS bound to PVA start the disassociation from PVA matrix. Although the weight loss does not have a big difference among PAQ composites, due to the addition of AE and QCS, the maximum decomposition temperature of PAQ composites as shown in **Figure 4b** increases as compared with pure PVA, which results in the increase of thermal stability of PAQ composites. The third stage between 300 and 380°C shows the highest weight loss of materials which are associated with the decomposition of molecular structure of PVA, AE, and QCS [38]. As shown in **Figure 4b**, in this stage, the maximum decomposition temperature is increased from 328.7°C for pure PVA to 335.5°C for PAQ3, 341.7°C for PAQ2, and 342.4°C for PAQ1. This means that the addition of AE and QCS increases the thermal stability of PAQ composites. Meanwhile, the decomposition rate of PAQ3 composites is greatly reduced as the increasing content of AE in the composite. The fourth stage between 380 and 450°C is associated with the decomposition of material proportion with higher crystalline structure in AE or QCS [42]. PAQ2 and PAQ3 containing higher amount of AE and QCS exhibit higher weight losses than pure PVA and PAQ. The above TGA analysis indicates that the addition of AE and QCS in PAQ composites is conducive to the enhancement of thermal stability of materials and beneficial to the moisture maintenance of PAQ composites.

http://dx.doi.org/10.5772/65476

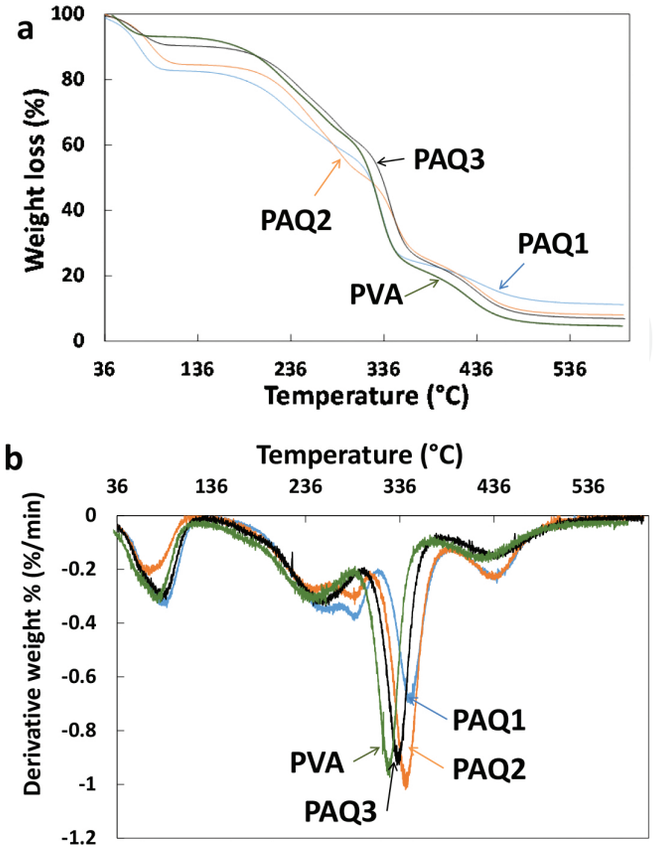

Figure 4. TGA (a) and DTG (b) curves of pure PVA and PAQ composites with different mass ratios of components: PAQ1, PVA:AE:QCS = 6:3:1; PAQ2, PVA:AE:QCS = 7:2:1; PAQ3, PVA:AE:QCS = 8:1:1.

The water absorbability of PAQ composites was investigated using two physiological solutions, PBS (pH 7.4) and HAc-NaAc (pH 5.0), at 37°C, to evaluate their potential to be used for fluid exchange and moisture maintenance because a real wound-healing process generally involves a variation of pH values from pH 5.0 for wound occurrence to pH 7.4 for wound closure [15, 16]. As shown in **Figure 5**, all the PAQ composites exhibit strong water absorbability over 10 times higher than their dry weight, as well as higher than pure PVA. This suggests that the incorporation of AE and QCS could significantly enhance the water absorbability of pure PVA. Owing to the maximum content of AE in PAQ1 composite, the maximum water absorption is 23.85 ± 0.76 for PAQ1 soaked in PBS, which means that this composite material could absorb 23.85 times its dry weight. As compared to PBS (pH 7.4), the PAQ composites exhibited a slight decline of water absorbability in HAc-NaAc (pH 5.0), partly because of the presence of QCS with a competency of proton donor neutralizing the acidic effect in HAc-NaAc buffer. Overall, the water absorption tends to be stable after soaking the composites for over 240 min and can be maintained until 720 min, which suggests that the optimal time to exchange new PAQ composites is somewhere between 240 and 720 min because old composites may lose persistent competency to absorb exudates from wound, whereas it can maintain the high moisture for wound. In consideration of both high water absorbability and relatively low cost resulted from less addition of AE and QCS, the composition of PAQ2 (PVA:AE:QCS, 7:2:1) may be the best choice.

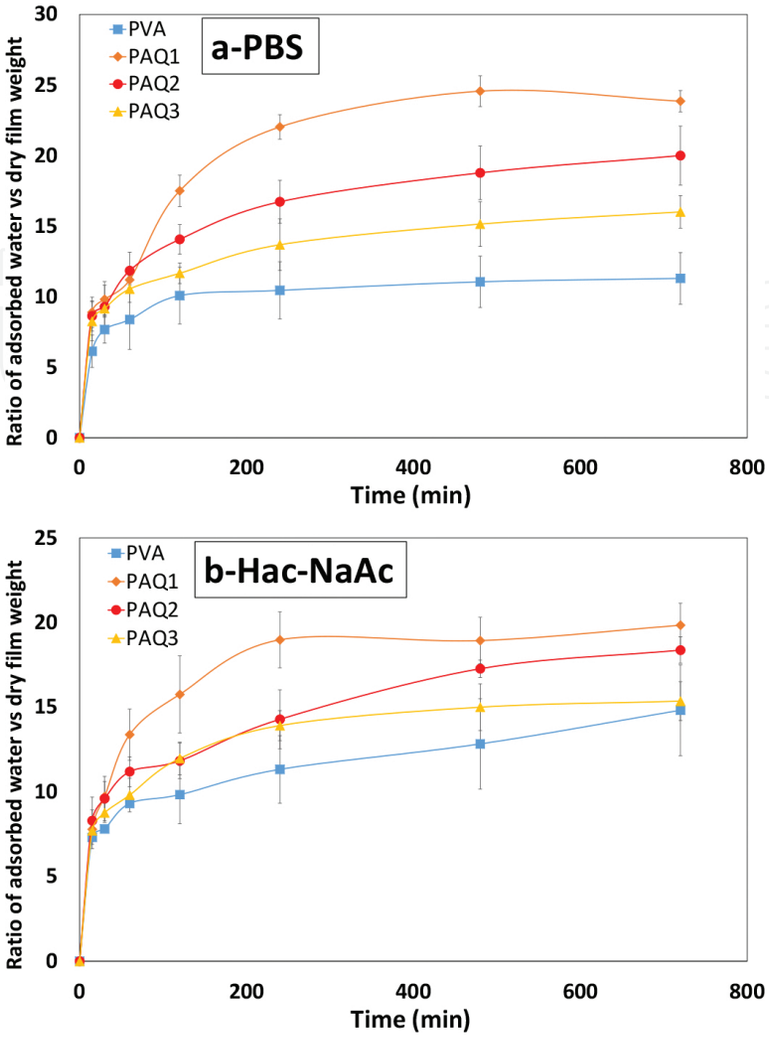

Figure 5. Water absorbability of pure PVA and PAQ composites with different mass ratios of components: PAQ1, PVA:AE:QCS = 6:3:1; PAQ2, PVA:AE:QCS = 7:2:1; PAQ3, PVA:AE:QCS = 8:1:1.

3.2. Antibacterial property and biocompatibility of wound-dressing composites

As shown in **Figure 6**, PAQ composites exhibit significant antibacterial property as compared to pure PVA because of the presence of QCS which is generally documented as a strong and bio-safe antibacterial agent. PAQ1 in **Figures 6e** and **f** exhibits a slightly better antibacterial property against both *E. coli* and *S. aureus* than PAQ2 and PAQ3, although their antibacterial effects are quite similar. This may be a reason of a higher amount of AE present in PAQ1 composite. All the PAQ composites show the excellent antibacterial outcomes over 99% after cell counting and calculation, which are 99.85% for PAQ1, 99.58% for both PAQ2 and PAQ3 against *E. coli*, and 99.80% for PAQ1, 99.69 for PAQ2, and 99.52% for PAQ3 against *S. aureus.* The proliferation of L929 mouse fibroblasts in the presence of pure PVA and PAQ composites over time is shown in **Figure 7**. No significant difference is present in the proliferation of L929 fibroblasts for PAQ composites, which suggests that the addition of QCS and AE to PVA matrix did not significantly influence the proliferation of L929 cells.

http://dx.doi.org/10.5772/65476

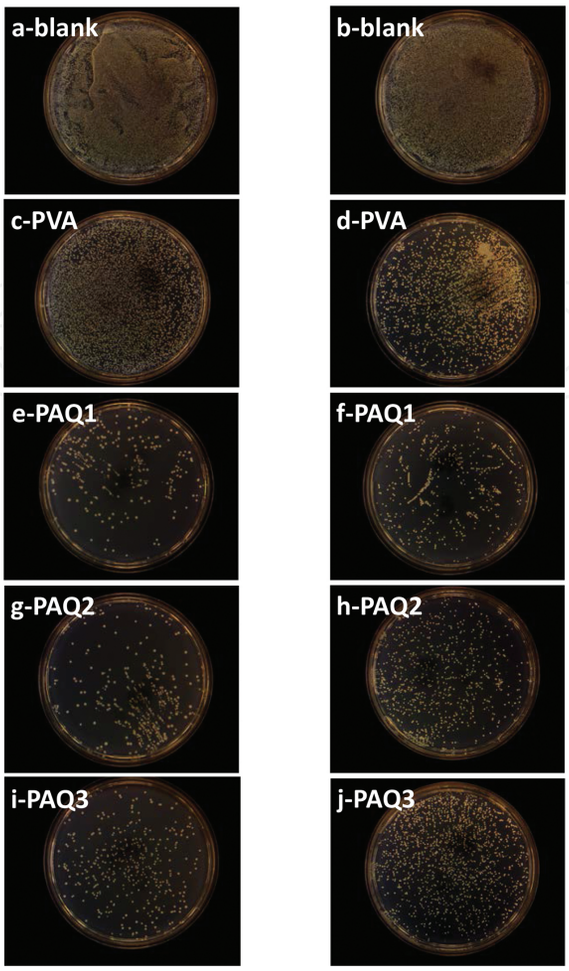

Figure 6. Antibacterial assays using *E. coli* (a, c, e, g, h) and *S. aureus* (b, d, f, h, j) for (c, d) pure PVA and PAQ composites with different mass ratios of components: (e, f) PAQ1, PVA:AE:QCS = 6:3:1; (g, h) PAQ2, PVA:AE:QCS = 7:2:1; (i, j) PAQ3, PVA:AE:QCS = 8:1:1. Images a and b are blank samples.

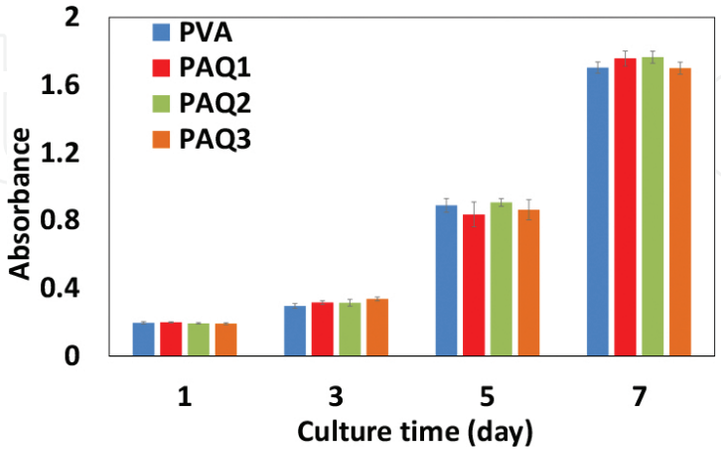

Figure 7. The effect of pure PVA and PAQ composites with different mass ratios of components on the proliferation of L929 mouse fibroblasts: PAQ1, PVA:AE:QCS = 6:3:1; PAQ2, PVA:AE:QCS = 7:2:1; PAQ3, PVA:AE:QCS = 8:1:1.

The attachment and morphology observation in the 3-day cultivation of HFCs on pure PVA and PAQ composites were analyzed as shown in **Figure 8**. All the samples show good attachment of HFCs on their substrates. A slightly preferable viability of HFCs is found in PAQ composites as compared to pure PVA, although no significant viability is present, suggesting that the impact of QCS against cell growth has been offset by AE which shows a potential of facilitating the growth of fibroblasts. L929 fibroblasts show a good morphology of extended shape on all the substrates, which suggests that either pure PVA or PAQ composites are satisfied substrates for the attachment and growth of L929 fibroblasts. In the light of the results from antibacterial assays and biocompatibility plus the analyses from SEM, FTIR, TGA, and water absorbability, considering the cost, the PAQ2 with a mass ratio of PVA:AE:QCS (7:2:1) exhibits relatively satisfactory properties and thereby it should become the optimal material composition.

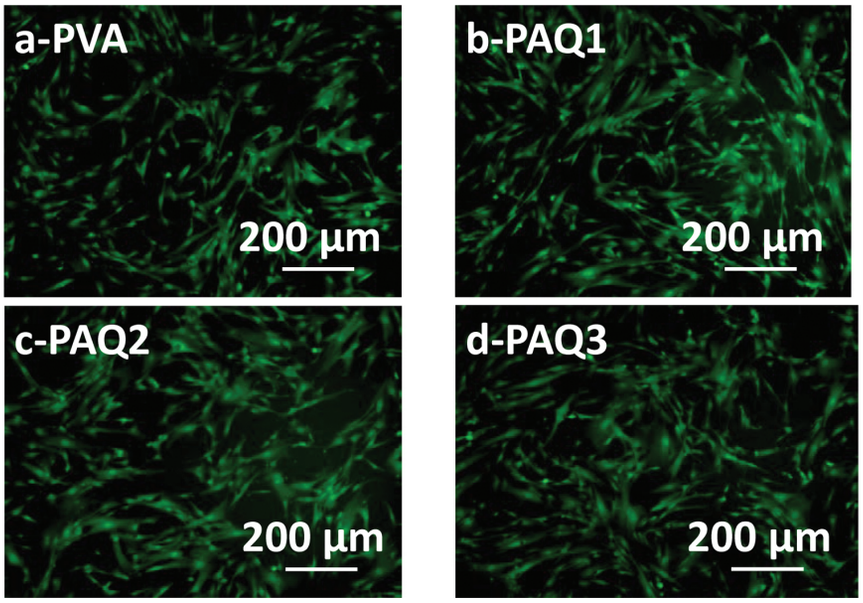

Figure 8. The attachment and morphology of HFCs on (a) pure PVA and PAQ composites with different mass ratios of components on the proliferation of L929 mouse fibroblasts on day 3: (b) PAQ1, PVA:AE:QCS = 6:3:1; (c) PAQ2, PVA:AE:QCS = 7:2:1; (d) PAQ3, PVA:AE:QCS = 8:1:1.

4. Conclusion

This work used a facile approach to prepare PVA/AE/QCS composites used as a multifunctional wound-dressing materials exhibiting strong antibacterial property, good moisture maintenance, and excellent biocompatibility for wound healing. The mass ratio of PAQ composites was controlled at three different levels of 6:3:1, 7:2:1, and 8:1:1 (PVA/AE/QCS). Material characterization of PAQ composites shows that PAQ composites possess a porous profile on both surface and cross-section areas with 3–60-μm pore size and a 3D porous network inside, in which PAQ composite with a mass ratio of 7:2:1 exhibits more homogeneous

porous structure. Such a homogeneous porous structure could effectively prevent the invasion of microorganism, as well as readily absorb extrudes from wound. FTIR and TGA results indicate that AE and QCS have been successfully bound to PVA matrix, and the addition of AE and QCS to PVA is conducive to the enhancement of thermal stability of composites. All the PAQ composites exhibit excellent water absorbability over 10 times higher than their dry weight in both PBS (pH 7.4) and HAc-NaAc buffer (pH 5.0). The PAQ composites exhibited an excellent antibacterial characteristic and a good biocompatibility of fibroblasts. In consideration of cost and results from material characterization plus antibacterial property and biocompatibility, the PAQ2 composite with a mass ratio of 7:2:1 exhibits relatively satisfactory thermal stability and antibacterial property plus fewer amounts of AE and QCS, and thereby it would become a competitive multifunctional wound dressing.

Acknowledgements

This work was financially supported by the National Natural Science Foundation of China no. 31570967 and 31370978; the Shenzhen Science and Technology Program no. JCYJ20140610152828698; the Shenzhen Peacock Program no. 110811003586331.

Author details

Yang Hu[1,2*], Yongjun Zhu[1] and Xin Zhou[1]

*Address all correspondence to: yang.hu@siat.ac.cn

1 Center for Human Tissue and Organs Degeneration and Shenzhen Key Laboratory of Marine Biomedical Materials, Institute of Biomedicine and Biotechnology, Shenzhen Institutes of Advanced Technology, Chinese Academy of Sciences, Shenzhen, Guangdong, China

2 Department of Plant and Soil Science, Fiber and Biopolymer Research Institute, Texas Tech University, Lubbock, TX, USA

References

[1] Thomas S. Wound Management and Dressings. London: The Pharmaceutical Press; 1990. p. 1–2.

[2] Dee KC, Puleo DA, Bizios R. An Introduction to Tissue-biomaterial Interactions. Hoboken, NJ: John Wiley and Sons; 2003. p. 1–10.

[3] Archana D, Dutta PK, Dutta J. Chitosan: A potential therapeutic dressing material for wound healing. In: Dutta PK, editors. Chitin and Chitosan for Regenerative Medicine. New York, NY: Springer; 2016. pp. 193–227. DOI: 10.1007/978-81-322-2511-9.

[4] Lionelli GT, Lawrence WT. 2003. Wound dressings. Surgical Clinics of North America. 2003; 83; 617–638. DOI: 10.1016/S0039-6109(02)00192-5.

[5] Boateng JS, Matthews KH, Stevens HNE, Eccleston GM. Wound healing dressings and drug delivery systems: a review. Journal of Pharmaceutical Sciences. 2008; 97: 2892–2923. DOI: 10.1002/jps.21210.

[6] Gonyon Jr DL, Zenn MR. Simple approach to the radiated scalp wound using INTEGRA skin substitute. Annals of Plastic Surgery. 2003; 50: 315–320.

[7] Sebastian K, Fellman J, Potter R, Bauer J, Searl A, DE Meringo A, Maquin B, DE Reydellet A, Jubb G, Moore M, Preininger R. EURIMA test guideline: in-vitro acellular dissolution of man-made vitreous silicate fibres. Glass Science and Technology. 2002; 75: 263–270.

[8] Puppi D, Chiellini F, Piras AM, Chiellini E. Polymeric materials for bone and cartilage repair. Progress in Polymer Science. 2010; 35: 403–440. DOI: 10.1016/j.progpolymsci.2010.01.006.

[9] McCullen SD, Hanson AD, Lucia LA, Loboa EG. Development and application of naturally renewable scaffold materials for bone tissue engineering. In: Lucia LA, Rojas OJ, editors. The Nanoscience and Technology of Renewable Biomaterials. India: Wiley; 2009. pp. 293–314.

[10] Bhattarai N, Matsen FA, Zhang M. PEG-grafted chitosan as an injectable thermoreversible hydrogel. Macromolecular Bioscience. 2005; 5: 107–111. DOI: 10.1002/mabi.200400140.

[11] Middleton JC, Tipton AJ. Synthetic biodegradable polymers as orthopedic devices. Biomaterials. 2000; 21: 2335–2346. DOI:10.1016/S0142-9612(00)00101-0.

[12] Temenoff JS, Mikos AG. Injectable biodegradable materials for orthopedic tissue engineering. Biomaterials. 2000; 21: 2405–2412. DOI:10.1016/S0142-9612(00)00108-3.

[13] Mohanty AK, Misra M, Hinrichsen G. Biofibres, biodegradable polymers and biocomposites: an overview. Macromolecular Materials and Engineering. 2000; 276: 1–24. DOI: 10.1002/(SICI)1439-2054(20000301)276:1<1::AID-MAME1>3.0.CO;2-W.

[14] Malafaya PB, Silva GA, Reisa RL. Natural–origin polymers as carriers and scaffolds for biomolecules and cell delivery in tissue engineering applications. Advanced Drug Delivery Reviews. 2007; 9: 207–233. DOI:10.1016/j.addr.2007.03.012.

[15] Hu Y, Catchmark JM. Integration of cellulases into bacterial cellulose: toward bioabsorbable cellulose composites. Journal of Biomedical Materials Research Part B: Applied Biomaterials. 2011; 97: 114–123. DOI: 10.1002/jbm.b.31792.

[16] Hu Y, Catchmark JM. In vitro biodegradability and mechanical properties of bioabsorbable bacterial cellulose incorporating cellulases. Acta Biomaterialia. 2011; 7: 2835–2845. DOI:10.1016/j.actbio.2011.03.028.

[17] Hu Y, Catchmark JM, Vogler, EA. Factors impacting the formation of sphere-like bacterial cellulose particles and their biocompatibility for human osteoblast growth. Biomacromolecules. 2013; 14: 3444–3452. DOI: 10.1021/bm400744a.

[18] Hu Y, Catchmark JM, Zhu Y, Abidi N, Zhou X, Wang J, Liang N. Engineering of porous bacterial cellulose toward human fibroblasts ingrowth for tissue engineering. Journal of Materials Research. 2014; 29: 2682–2693. DOI: http://dx.doi.org/10.1557/jmr.2014.315.

[19] Hu Y, Zhu Y, Zhou X, Ruan C, Pan H, Catchmark JM. Bioabsorbable cellulose composites prepared by an improved mineral-binding process for bone defect repair. Journal of Materials Chemistry B. 2016; 4: 1235–1246. DOI: 10.1039/C5TB02091C.

[20] Hu Y, Catchmark JM. Formation and characterization of spherelike bacterial cellulose particles produced by Acetobacter xylinum JCM 9730 strain. Biomacromolecules. 2010; 7: 1727–1734. DOI: 10.1021/bm100060v.

[21] Lin J, Yu W, Liu X, Xie H, Wang W, Ma X. In vitro and in vivo characterization of alginate-chitosan-alginate artificial microcapsules for therapeutic oral delivery of live bacterial cell. Journal of Bioscience and Bioengineering. 2008; 105: 660–665. DOI:10.1263/jbb.105.660.

[22] Huang S, Liang N, Hu Y, Zhou X, Abidi N. Polydopamine-assisted surface modification for bone biosubstitutes. BioMed Research International. 2016: 1–9. DOI: http://dx.doi.org/10.1155/2016/2389895.

[23] Jayakumar R, Prabaharan M, Kumar PS, Nair SV, Tamura H. Biomaterials based on chitin and chitosan in wound dressing applications. Biotechnology Advances. 2011; 29: 322–337. DOI:10.1016/j.biotechadv.2011.01.005.

[24] Jayakumar R, Menon D, Manzoor K, Nair SV, Tamura H. Biomedical applications of chitin and chitosan based nanomaterials—a short review. Carbohydrate Polymers. 2010; 82: 227–232. DOI:10.1016/j.carbpol.2010.04.074.

[25] Mi FL, Shyu, SS, Wu YB, Lee ST, Shyong JY, Huang RN. Fabrication and characterization of a sponge-like asymmetric chitosan membrane as a wound dressing. Biomaterials. 2001; 22: 165–173. DOI:10.1016/S0142-9612(00)00167-8.

[26] Pakravan M, Heuzey MC, Ajji A. A fundamental study of chitosan/PEO electrospinning. Polymer. 2011; 52: 4813–4824. DOI:10.1016/j.polymer.2011.08.034.

[27] Jia Y, Gong J, Gu X, Kim H, Dong J, Shen X. Fabrication and char-acterization of poly (vinyl alcohol)/chitosan blend nanofibers produced by electrospinning method. Carbohydrate Polymers. 2007; 67: 403–409. DOI:10.1016/j.carbpol.2006.06.010.

[28] Xu J, Zhang J, Gao W, Liang H, Wang H, Li J. Preparation of chitosan/PLA blend micro/nanofibers by electrospinning. Materials Letters. 2009; 63: 658–660. DOI:10.1016/j.matlet.2008.12.014.

[29] Chen Z, Mo X, Qing F. Electrospinning of collagen–chitosan complex. Materials Letters. 2007; 61: 3490–3494. DOI:10.1016/j.matlet.2006.11.104.

[30] Xu F, Weng B, Gilkerson R, Materon LA, Lozano K. Development of tannic acid/chitosan/pullulan composite nanofibers from aqueous solution for potential applications as wound dressing. Carbohydrate polymers. 2015; 115: 16–24. DOI:10.1016/j.carbpol.2014.08.081.

[31] Lin WC, Lien CC, Yeh HJ, Yu CM, Hsu SH. Bacterial cellulose and bacterial cellulose–chitosan membranes for wound dressing applications. Carbohydrate Polymers. 2013; 94: 603–611. DOI:10.1016/j.carbpol.2013.01.076.

[32] Davis RH, Donato JJ, Hartman GM, Haas RC. Anti-inflammatory and wound healing activity of a growth substance in Aloe vera. Journal of the American Podiatric Medical Association. 1994; 84: 77. DOI: 10.7547/87507315-84-2-77.

[33] Choi SW, Son BW, Son YS, Park YI, Lee SK, Chung MH. The wound – healing effect of a glycoprotein fraction isolated from Aloe vera. British Journal of Dermatology. 2001; 145: 535–545. DOI: 10.1046/j.1365-2133.2001.04410.x.

[34] Farzadinia P, Jofreh N, Khatamsaz S, Movahed A, Akbarzadeh S, Mohammadi M, Bargahi A. Anti-inflammatory and Wound Healing Activities of Aloe vera, Honey and Milk Ointment on Second-Degree Burns in Rats. The International Journal of Lower Extremity Wounds. 2016; 15: 241–247. DOI: 10.1177/1534734616645031.

[35] Tummalapalli M, Berthet M, Verrier B, Deopura BL, Alam MS, Gupta B. Composite wound dressings of pectin and gelatin with Aloe vera and curcumin as bioactive agents. International Journal of Biological Macromolecules. 2016; 82: 104–113. DOI:10.1016/j.ijbiomac.2015.10.087.

[36] Rees A, Powell LC, Chinga-Carrasco G, Gethin DT, Syverud K, Hill KE, Thomas DW. 3D bioprinting of carboxymethylated-periodate oxidized nanocellulose constructs for wound dressing applications. BioMed research international. 2015; 2015: 1–7. DOI: 10.1155/2015/925757.

[37] Anicuta SG, Dobre L, Stroescu M, Jipa I. Fourier transform infrared (FTIR) spectroscopy for characterization of antimicrobial films containing chitosan. Analele Universită Ńii din Oradea, Fascicula Ecotoxicologie, Zootehnie şi Tehnologii de Industrie Alimentară. 2010: 1234-1240. Available from: https://www.researchgate.net/profile/Iuliana_Jipa/publication/267248659_Fourier_Transform_Infrared_(FTIR)_spectroscopy_for_characterization_of_antimicrobial_films_containing_chitosan/links/544de4df0cf2bcc9b1d8f44b.pdf [Accessed: 2016-09-22].

[38] Pereira R, Carvalho A, Vaz DC, Gil MH, Mendes A, Bártolo P. Development of novel alginate based hydrogel films for wound healing applications. International Journal of Biological Macromolecules. 2013; 52: 221–230. DOI: 10.1016/j.ijbiomac.2012.09.031.

[39] El Miri N, Abdelouahdi K, Zahouily M, Fihri A, Barakat A, Solhy A, El Achaby M. Bionanocomposite films based on cellulose nanocrystals filled polyvinyl alcohol/chitosan polymer blend. Journal of Applied Polymer Science. 2015; 132: 1–13. DOI: 10.1002/app.42004.

[40] Abidi N, Cabrales L, Haigler CH. Changes in the cell wall and cellulose content of developing cotton fibers investigated by FTIR spectroscopy. Carbohydrate Polymers. 2014; 100: 9–16. DOI:10.1016/j.carbpol.2013.01.074.

[41] Lewandowska K. Miscibility and thermal stability of poly (vinyl alcohol)/chitosan mixtures. Thermochimica Acta. 2009; 493: 42–48. DOI: 10.1016/j.tca.2009.04.003.

[42] Mohamed RR, Elella MHA, Sabaa MW. Synthesis, characterization and applications of N-quaternized chitosan/poly (vinyl alcohol) hydrogels. International Journal of Biological Macromolecules. 2015; 80: 149–161. DOI: 10.1016/j.ijbiomac.2015.06.041.

IntechOpen